DOI: 10.15255/KUI.2017.028
KUI-3/2018
Original scientific paper
Received July 3, 2017
Accepted October 27, 2017

Mesoporous $PtSnO_2$/C Catalyst with Enhanced Catalytic Activity for Ethanol Electro-oxidation

S. Y. Chen,[a] *L. Shi*,[a,b*] and *L. Wang*[c]

[a] School of Chemistry and Chemical Engineering, Shihezi University, Shihezi, Xinjiang, 832 000, P.R. China
[b] Key Laboratory for Green Processing of Chemical Engineering of Xinjiang Bingtuan, Shihezi, Xinjiang, 832 000, P.R. China
[c] Shandong University of Traditional Chinese Medicine, Shandong, 250 355, P.R. China

Abstract

In this paper, we report the synthesis, characterization, and electrochemical evaluation of a mesoporous $PtSnO_2$/C catalyst, called $PtSnO_2$(M)/C, with a nominal Pt : Sn ratio of 3 : 1. Brunauer–Emmett–Teller and transmission electron microscopy characterizations showed the obvious mesoporous structure of SnO_2 in $PtSnO_2$(M)/C catalyst. X-ray photoelectron spectroscopy analysis exhibited the interaction between Pt and mesoporous SnO_2. Compared with Pt/C and commercial $PtSnO_2$/C catalysts, $PtSnO_2$(M)/C catalyst has a lower active site, but higher catalytic activity for ethanol electro-oxidation reaction (EOR). The enhanced activity could be attributed to Pt nanoparticles deposited on mesoporous SnO_2 that could decrease the amount of poisonous intermediates produced during EOR by the interaction between Pt and mesoporous SnO_2.

Keywords

Ethanol electro-oxidation reaction, Pt-Sn catalyst, mesoporous SnO_2, enhanced catalytic activity

1 Introduction

The direct ethanol fuel cell (DEFC) has been extensively investigated because ethanol is regarded as one of the potential fuels for H_2 and methanol in polymer electrolyte membrane fuel cell applications. However, the ethanol oxidation reaction (EOR) that occurs in the fuel cell anode is slow and incomplete, thus reducing the anode catalytic performance of DEFC. Many investigations have been conducted to improve the anode performance of DEFC. The Pt-Sn catalyst was reported to be the most effective catalyst for EOR compared with other Pt-based binary catalysts[1,2] because of its enhanced ability to break the C–C bond and improved resistance to poison from CO-like intermediates produced during ethanol oxidation reaction.[3–5] However, the activity of Pt-Sn catalyst still cannot satisfy the criteria for commercial DEFC anode catalyst. Therefore, catalytic performance should be improved further by redesigning Pt-Sn catalyst.

The role of SnO_2 on the enhanced EOR activity of Pt-Sn catalysts has been extensively investigated.[6,7] Recently, some investigators have reported that SnO_2 species can produce hydroxy radical species at lower potential than Pt. Thus, CO-like intermediate residues react with hydroxy radical species in the vicinity of Pt particles to free Pt active sites based on the bifunctional mechanism.[8,9] SnO_2 also improves the cycling stability of Pt-Sn catalysts because of its corrosion-resistant property. However, some investigations determined that SnO_2 nanoparticles are fully coated with the Pt layer. These nanoparticles cannot produce hydroxy radical species to increase the CO tolerance of the catalyst based on the bifunctional mechanism.[10] Pt particles are poisoned by CO-like species if no direct contact occurs between Pt particles and SnO_2.[11] Several studies have recently focused on $PtSnO_2$ systems that exhibit high catalytic activity for ethanol oxidation. *Zhang et al.*[12] determined that Pt supported on SnO_2 flower-shaped catalyst demonstrates high electrocatalytic activity and long-term cycle stability because of the multi-dimensional active sites and radial channels of liquid diffusion. *Zhang et al.*[11] showed that Pt/(CNT@SnO_2) catalysts exhibit significantly higher catalytic activity and CO tolerance for ethanol electro-oxidation than Pt/CNT. Pt-Sn catalysts can improve EOR activity by alloying with a third metal (Ir or Rh).[5,13] Ternary $PtRhSnO_2$ electrocatalyst for ethanol oxidation can be significantly improved because SnO_2 supplies hydroxy radical species, whereas Rh can be induced to break the C–C bond at room temperature.[13] *Li et al.*[5] determined that $PtIrSnO_2$/C catalyst with high Ir content exhibits outstanding catalytic properties for EOR and good selectivity toward complete oxidation of ethanol to CO_2. However, Rh and Ir are rare and costly precious metals. It has been suggested that some non-noble metal oxides possess good capacity for preventing CO poisoning.[14,15] Therefore, in this work, we will try to enhance the performance of Pt catalyst for ethanol oxidation through forming mesoporous $PtSnO_2$ nanoparticles.

Although considerable effort has been exerted to prepare mesoporous SnO_2 nanomaterials because of their excel-

* Corresponding author: Lei Shi
e-mail: 16105807@qq.com

lent properties for application in Li-ion batteries and gas sensors,[16,17] the catalytic behaviour of mesoporous SnO_2 toward EOR has been rarely studied. In the present work, we prepared C-supported electrocatalysts that consist of a mesoporous SnO_2 core decorated with Pt nanoislands *via* modified polyol method. We hypothesized that this special catalyst structure will increase the catalytic activity and CO tolerance of Pt to ethanol oxidation.

2 Experiment details

2.1 Materials

$H_2PtCl_6 \cdot 6\ H_2O$, $SnCl_2 \cdot 2\ H_2O$, $Na_2SnO_3 \cdot H_2O$, oleic acid, ethylene glycol (EG), H_2SO_4, ethanol, and Nafion were purchased from Sigma-Aldrich, St. Louis, Mo, USA. Vulcan XC72R carbon black ($S_{BET} = 250\ m^2\ g^{-1}$) was purchased from Cabot Corporation, Boston, MA, USA. All chemicals were of analytical grade and used as received without further purification.

2.2 Synthesis of mesoporous SnO_2

Mesoporous SnO_2 was synthesized *via* a water-evaporating process that was previously reported in.[18] In this process, 0.45 g $Na_2SnO_3 \cdot 3\ H_2O$ was added into 5 ml distilled water in an open container. After $Na_2SnO_3 \cdot 3\ H_2O$ had completely dissolved, 25 ml oleic acid was added to the Na_2SnO_3 solution. The container was maintained at 150 °C for 5 h at ambient pressure, and then allowed to cool to room temperature naturally. The resulting precipitate was filtered, washed, and dried at 60 °C for 12 h. Finally, the solid was further treated at 300 °C in air for 2 h to obtain SnO_2 mesoporous nanomaterials.

2.3 Synthesis of $PtSnO_2$(M)/C catalyst

The appropriate amount of mesoporous SnO_2 was first dissolved in 50 ml EG and sonicated for 0.5 h. The appropriate amount of $H_2PtCl_6 \cdot 6\ H_2O$ was then added. The solution was heated to 130 °C and maintained at this temperature for 2 h. The solution cooled down to 60 °C. Afterward, the appropriate amount of XC72R carbon black was added to the solution, an aqueous solution of HCl (1.5 M) was added to adjust the pH of the solution to approximately 1. The solution was then stirred for another 6 h and cooled down to room temperature. The obtained mixture was filtered, washed, and dried.

For comparison, $PtSnO_2$(N)/C catalyst was synthesized in a manner similar to that of $PtSnO_2$(M)/C catalyst, except for the preparation of SnO_2 nanoparticles. SnO_2 nanoparticles were obtained through the following steps. The appropriate amount of $SnCl_2 \cdot 2H_2O$ was firstly dissolved in 50 ml EG and 1 ml water to form a solution. The solution was then heated to 180 °C, maintained at this temperature for 2 h, and cooled to room temperature. Pt/C was also prepared without adding SnO_2. The mass fraction of Pt in the catalyst was $w(Pt) = 0.20$.

2.4 Characterization of catalysts

Brunauer–Emmett–Teller (BET) surface area analysis was performed from the nitrogen adsorption isotherms at 77 K using an ASAP 2020 physisorption analyser (Micromeritics Instrument Corporation, Norcross, GA, USA). All samples were degassed at 110 °C under vacuum for 6 h. Average pore diameter (d_{av}) and pore volume were calculated based on the Barrett–Joyner–Halenda (BJH) method. Powder X-ray diffraction (XRD) data were collected on a D8 ADVANCE X-ray diffractometer (Bruker Biosciences Corporation, Billerica, MA, USA) using Cu Kα irradiation ($\lambda = 1.5406$ Å) as source at 40 kV and 40 mA. Transmission electron microscopy (TEM) experiments were conducted using Tecnai F30 field emission transmission electron microscope (FEI, Hillsboro, OR, USA). Inductively coupled plasma atomic emission spectroscopy (ICP-AES) was conducted using the TCAP 6000 SERICS ICP emission spectrometer. X-ray photoelectron spectroscopy (XPS) analyses were performed on ESCA 3400 (Kratos Analytical Ltd., Manchester, UK) equipped with Al and Mg sources (1486.6 eV, 12 kV, 300 W). The base pressure of the system was $5 \cdot 10^{-7}$ Pa, and the measurements were conducted at $8 \cdot 10^{-7}$ Pa to $1 \cdot 10^{-6}$ Pa. For each catalyst, a survey spectrum was collected before high-resolution spectra were recorded. Deconvolutions of XPS spectra were conducted using the software XPS Peak 4.1.

2.5 Electrochemical measurements

A model 760B potentiostat/galvanostat (CH Instruments, Inc., Austin, TX, USA) was used for electrochemical measurements in a standard three-compartment electrochemical cell. All electrochemistry experiments were conducted at room temperature. The working electrode was a glass C disk with a diameter of 4 mm held in a Teflon cylinder. A Pt foil counter electrode and a saturated calomel reference electrode (SCE) (separated by an electrolyte salt bridge) were used. The working electrode was prepared as follows: Firstly, 5 mg catalyst was mixed with 1 ml ethanol and 5 µl 5 % Nafion solution. The mixture was ultrasonically suspended to obtain ink slurry. Then, 40 µl slurry was spread on the working electrode to form a thin layer. Linear sweep voltammetry (LSV) at a scan rate of 5 $mV\ s^{-1}$ and chronoamperometry (CA) experiment at a scan rate of 50 $mV\ s^{-1}$ were conducted in the electrolyte of 0.5 M H_2SO_4, which contained 1 M ethanol. Cyclic voltammetry (CV) experiments were conducted in the electrolyte of 0.5 M H_2SO_4 at a scan rate of 50 $mV\ s^{-1}$. Measurements were performed at room temperature, and the potentials reported in this paper were referenced to those of an SCE.

3 Results and discussion

The XRD patterns of the obtained SnO_2 sample are shown in Fig. 1a. All peaks can be attributed to the diffraction of the tetragonal SnO_2 (JCPDS Card No. 41-1445). The peaks located at approximately 27°, 34°, 52°, 65°, and 72° correspond to the (110), (101), (200), (211), (301), and (202) faces of the tetragonal SnO_2, respectively.[16] Fig. 1b shows

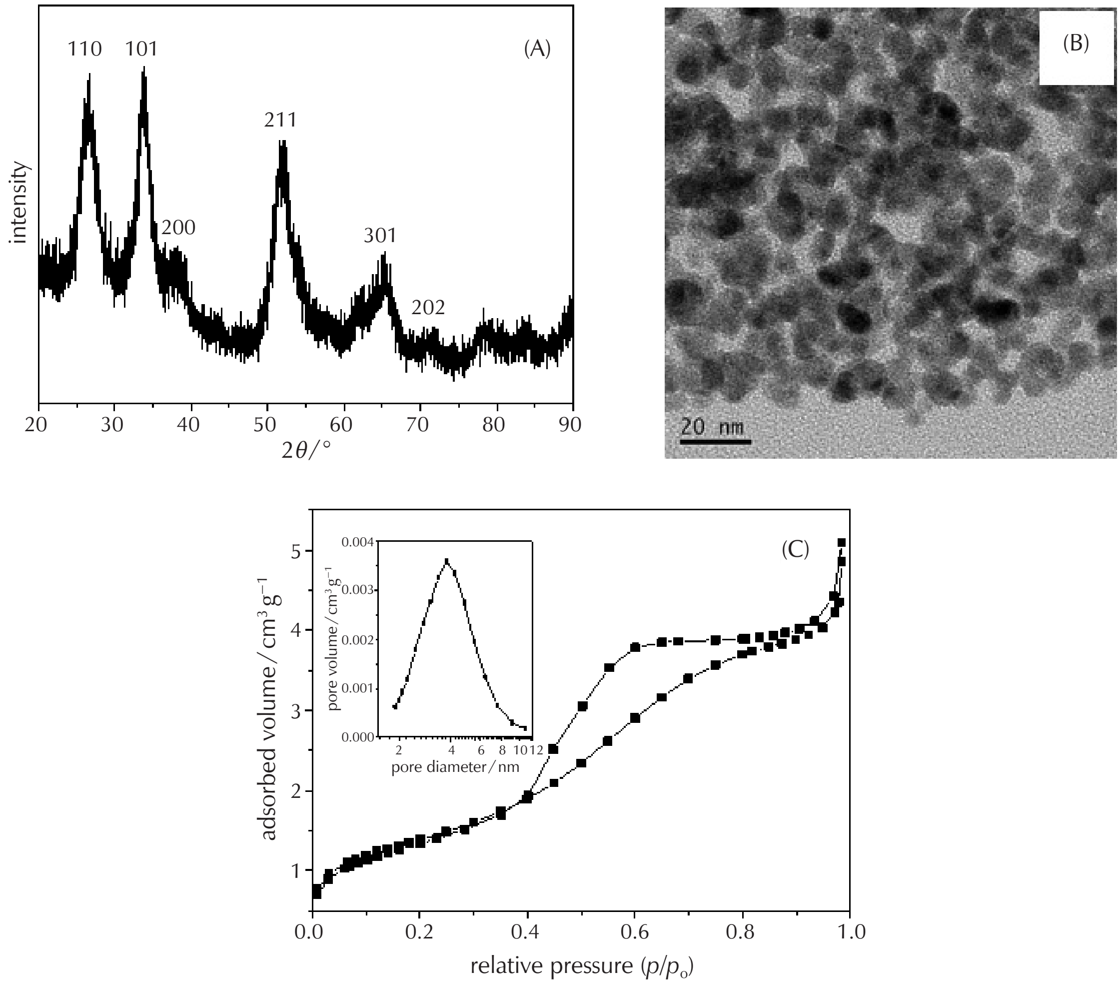

Fig. 1 – (A) XRD pattern, (B) TEM image, and (C) BET image of the as-synthesized mesoporous SnO_2 nanomaterials

a typical TEM image of the SnO_2 sample. Fig. 1c shows the nitrogen adsorption/desorption isotherm and the BJH pore size distribution plot of the as-synthesized mesoporous SnO_2 nanomaterials. A classic type IV isotherm with a type H3 hysteresis loop resulted from the quadratic capillary condensation at an intermediate relative pressure (p/p_o) of 0.4 to 0.9, thus indicating the presence of a highly mesoporous structure.[19] The surface area for SnO_2 is 109 $m^2\,g^{-1}$. Such structure produces a unimodal pore size distribution of 3.8 nm, which was calculated from the desorption branch of the nitrogen adsorption isotherm.

Fig. 2 shows the TEM images of Pt/C, $PtSnO_2$(N)/C, and $PtSnO_2$(M)/C catalysts. From Figs. 2a and 2c, it was observed that Pt and $PtSnO_2$(N) nanoparticles are well dispersed on XC72R carbon black. The size of Pt nanoparticles (NPs) in Pt/C ranges from 1.5 to 4.0 nm, with an average value of 2.0 nm (Fig. 2b). The size of Pt NPs in $PtSnO_2$(N)/C with diameters from 1.0 to 4.5 nm, had an average value of 2.7 nm (Fig. 2d). For $PtSnO_2$(M)/C catalysts, size dispersion is difficult to determine because of their irregular shape. The selective deposition of Pt on mesoporous SnO_2 results in poor dispersion (Fig. 2e). The high-resolution (HR) TEM micrograph further shows that the size of Pt nanoparticles is estimated to be 1.5 to 7.5 nm, with a mean value of 4.3 nm (Fig. 2f), which is larger than those of Pt/C and $PtSnO_2$(N)/C catalysts (Fig. 3c). In addition, several researchers have reported that the ideal particle size for Pt and Pt-based electrocatalysts is within the range of 2.0 to 4.0 nm.[20] Therefore, the selected method can be suitable for preparing Pt-based catalysts.

Fig. 3 shows typical HRTEM images of $PtSnO_2$(N)/C and $PtSnO_2$(M)/C catalysts. A 0.227 nm *d*-spacing was assigned to Pt (111), whereas a 0.335 nm *d*-spacing was assigned to SnO_2 (110). Compared with the lattice constant of pure Pt, the crystal lattice of Pt in the $PtSnO_2$(N)/C and $PtSnO_2$(M)/C samples remains unchanged (Figs. 3b and 3d). This phenomenon indicates that the SnO_2 additive has no effect on the crystal lattice of Pt. In the HRTEM image of $PtSnO_2$(N)/C, SnO_2 nanoparticles are observed in the vicinity of Pt particles (Fig. 3a). In the HRTEM image of $PtSnO_2$(M)/C (Figs. 3c and 3d), crystalline SnO_2 nanoislands support and finely deposited Pt nanoislands are obviously presented. Pt and SnO_2 nanoislands have more contact in $PtSnO_2$(M)/C.

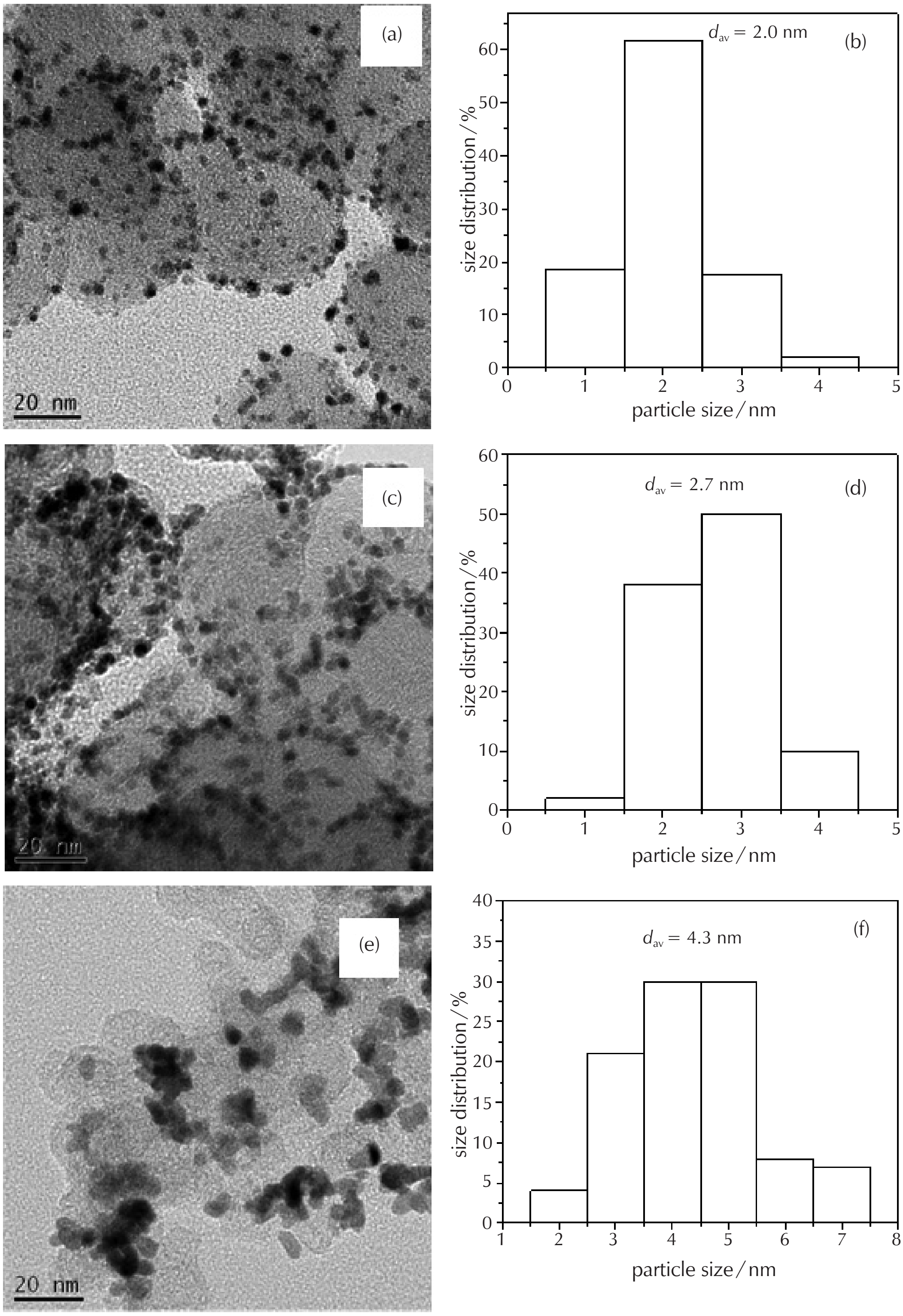

Fig. 2 – TEM images and size distribution of Pt nanoparticles in Pt/C (a,b), $PtSnO_2$(N)/C (c,d), and $PtSnO_2$(M)/C catalysts (e,f)

The valences of Pt for Pt/C, $PtSnO_2$(N)/C, and $PtSnO_2$(M)/C catalysts were determined by XPS, as shown in Fig. 4a. Three different valences of Pt (0), Pt (II), and Pt (IV) are observed in the three samples, which are characterized by the doublet binding energy of Pt $4f_{7/2}$ and Pt $4f_{5/2}$.[21] Compared with the peaks of Pt $4f_{5/2}$ in Pt/C, the change in $PtSnO_2$(N)/C value is negligible. However, the Pt $4f_{5/2}$ peaks of $PtSnO_2$(M)/C are approximately 0.4 eV higher than those of Pt/C, which further demonstrates the interaction between Pt and mesoporous SnO_2. This result was obtained

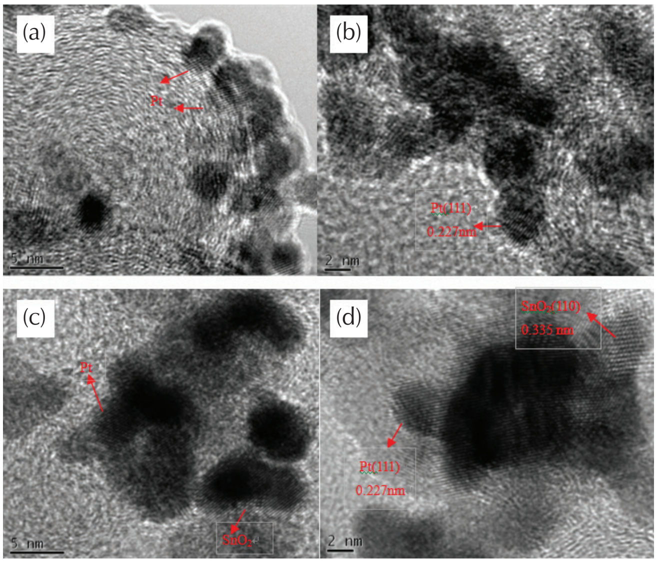

Fig. 3 – HRTEM images of (a and b) $PtSnO_2$(N)/C and (c and d) $PtSnO_2$(M)/C catalysts

through HRTEM. In addition, the high-resolution XPS spectra of Sn_{3d} in $PtSnO_2$(N)/C and $PtSnO_2$(M)/C are shown in Fig. 4b. The XPS spectrum ranging from 482 eV to 500 eV that are assigned to two peaks, *i.e.*, the Sn $3d_{5/2}$ peak centred at 487.3 eV and the Sn $3d_{3/2}$ peak at 495.9 eV, agrees well with those reported in literature.[22,23] All Sn $3d_{5/2}$ signals are deconvoluted into two components that correspond to Sn(II) (485.6 eV) and Sn(IV) (487.4 eV).[24,25] The Sn $3d_{5/2}$ peaks of Sn(II) (485.9 eV) and Sn(IV) (487.5 eV) are 0.2 eV higher than those of $PtSnO_2$(N)/C for Sn(II) (485.6 eV) and Sn(IV) (487.3 eV). The change in Sn value in $PtSnO_2$(M)/C catalyst may be attributed to the change in its electronic structure.

ICP-AES was conducted to determine the actual content of the elements in the catalysts. As shown in Table 1, the mass fraction of Pt is 19.8 % and 19.4 %, whereas that of Sn is 4.2 % and 4.3 % in $PtSnO_2$(N)/C and $PtSnO_2$(M)/C catalysts, respectively. This result reveals that neither Pt nor Sn is dissolved during the preparation process. Fig. 5 shows the XRD patterns of Pt/C, $PtSnO_2$(N)/C, and $PtSnO_2$(M)/C catalysts. For the three samples, the peak at approximately 25° is attributed to the diffraction at the (002) plane of the hexagonal structure of Vulcan XC72R carbon black. The other four diffraction peaks are characteristic of the face-centred cubic structure of Pt, and correspond to the planes of Pt (111), Pt (200), Pt (220), and Pt (311) at approximately 40°, 46°, 67°, and 81°, respectively. These results were in good agreement with the Pt standard (JCPDS PDF#04-0802) without any shift, which further indicated the absence of alloy formation between Pt and Sn and the presence of segregated Pt and SnO_2 phases in $PtSnO_2$(M)/C and $PtSnO_2$(N)/C. In addition, the peaks in Pt/C and $PtSnO_2$(N)/C catalysts are broader and weaker than those in $PtSnO_2$(M)/C catalyst, thus indicating the small size and low relative crystallinity of Pt nanoparticles in Pt/C and $PtSnO_2$(N)/C catalysts.[23] This result matches well with the TEM analysis.

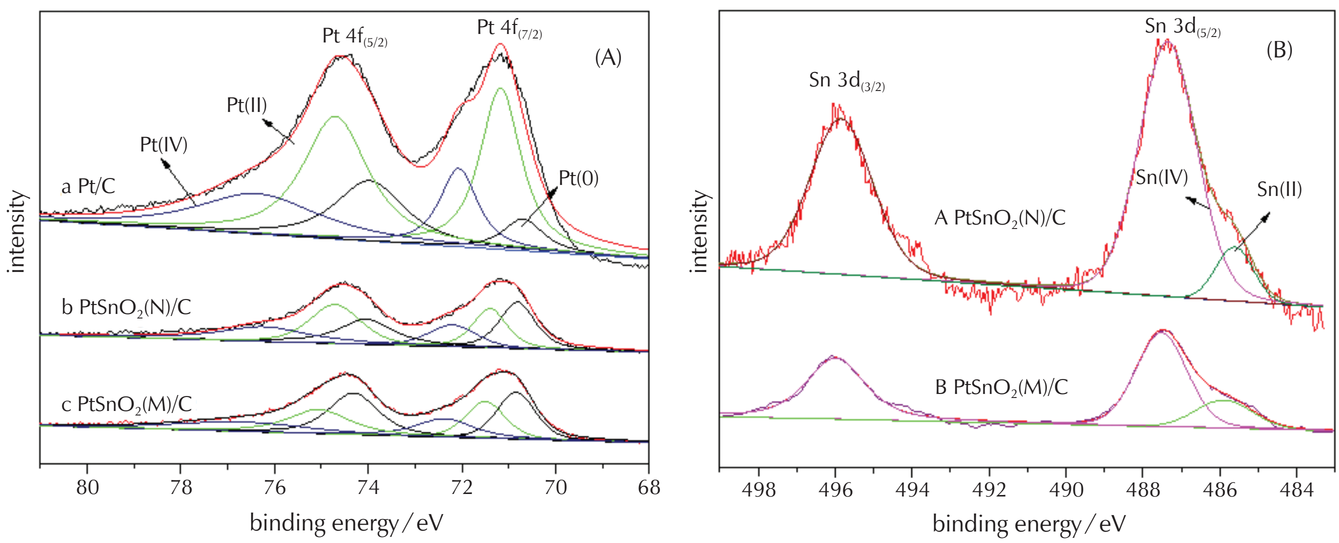

Fig. 4 – HR XPS spectra of (A) Pt 4f of Pt/C, $PtSnO_2$(N)/C, and $PtSnO_2$(M)/C catalysts; and (B) Sn 3d of $PtSnO_2$(N)/C and $PtSnO_2$(M)/C catalysts

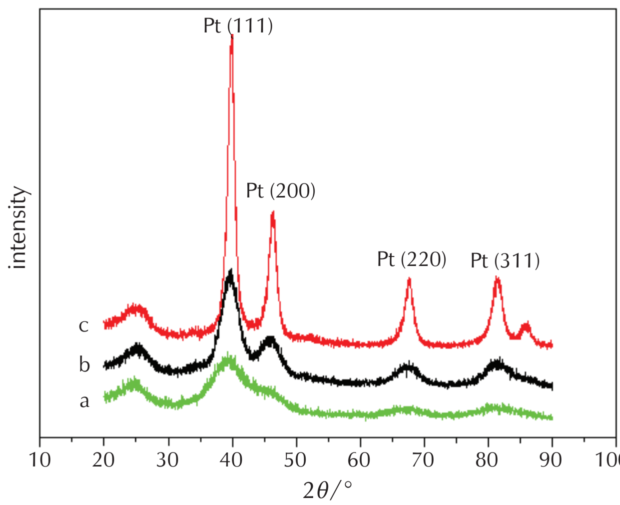

Fig. 5 – Wide-angle XRD patterns of (a) Pt/C, (b) $PtSnO_2$(N)/C, and (c) $PtSnO_2$(M)/C catalysts

Table 1 – Element components of $PtSnO_2$(N)/C and $PtSnO_2$(M)/C catalysts

Catalyst	Nominal content		Actual content		$(Sn/Pt)_{actu}$
	w(Pt) / %	w(Sn) / %	w(Pt) / %	w(Sn) / %	
$PtSnO_2$(N)/C	19.96	4.15	19.8	42	0.343
$PtSnO_2$(M)/C	19.96	4.15	19.4	4.3	0.349

Fig. 6 shows the CV curves of Pt/C, $PtSnO_2$(N)/C, and $PtSnO_2$(M)/C electrodes in 0.5 M H_2SO_4 electrolyte at room temperature. Well-defined hydrogen adsorption-desorption peaks are observed in the potential region of −0.24 to 0.06 V. The hydrogen adsorption/desorption and oxide reduction processes can be used to qualitatively evaluate electrode surface structures.[26] We observed that the areas of hydrogen adsorption and desorption peaks in the order of Pt/C > $PtSnO_2$(N)/C > $PtSnO_2$(M)/C catalysts. However, in the double-layer capacitance region of $PtSnO_2$(M)/C catalyst, between 0.1 and 0.4 V, a less capacitive current was observed than $PtSnO_2$(N)/C, indicating the conductivity of $PtSnO_2$(M)/C is better than $PtSnO_2$(N)/C. This effect could be due to the better conductivity of mesoporous SnO_2 than SnO_2 nanoparticles. The oxide reduction peak at over 0.5 V for $PtSnO_2$(M)/C catalyst is larger than Pt/C, indicating more Pt active sites in $PtSnO_2$(M)/C catalyst. The contradiction may be attributed to the fact that some of the Pt active sites for hydrogen and adsorption are blocked by SnO_2.[21] The result suggests that the Pt nanoparticles may have been covered by mesoporous SnO_2 successfully. The electrochemically active surface area (ECSA) is calculated by integrating the charge passing through the electrode during the hydrogen adsorption/desorption process after correcting the double layer formation. The charge required to oxidize a hydrogen monolayer is 0.21 mC cm^{-2}.[27] The value of ECSA can be obtained through Eq. (1):

$$\text{ECSA} / \text{m}^2\,\text{g}^{-1} = \frac{Q / \text{mC}}{0.21\ \text{mC cm}^{-2} \cdot m(\text{Pt}) / \text{mg}} \times 10^{-1}. \qquad (1)$$

The specific ECSA of $PtSnO_2$(M)/C is 19.69 m^2 g^{-1}, which is ~44 % that of Pt/C electrocatalyst (44.98 m^2 g^{-1}), and ~67 % that of $PtSnO_2$(N)/C (29.73 m^2 g^{-1}). The lower ECSA of $PtSnO_2$(M)/C catalyst can be attributed to its large nanoparticle size. Some Pt active sites for hydrogen adsorption are blocked by SnO_2.[21,28]

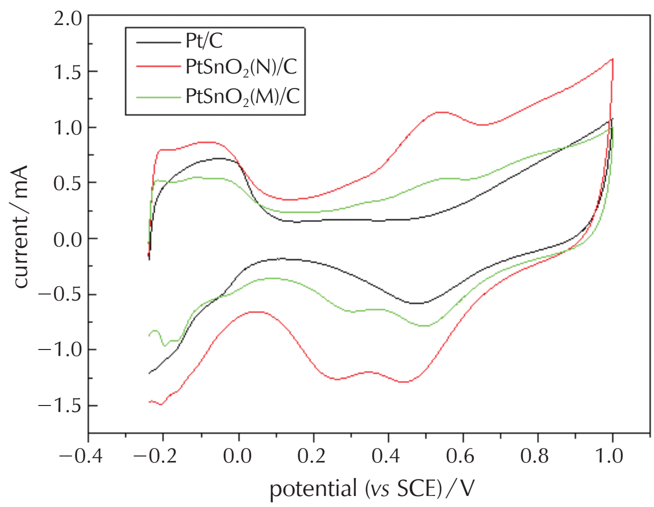

Fig. 6 – CVs of Pt/C, $PtSnO_2$(N)/C, and $PtSnO_2$(M)/C electrodes were measured in 0.5 M H_2SO_4 electrolyte at room temperature at a scan rate of 50 mV s^{-1}

To evaluate the EOR catalysis of $PtSnO_2$(M)/C catalyst, LSV at a scan rate of 5 mV s^{-1} was conducted. As shown in Fig. 7a, the onset potentials of Pt/C, $PtSnO_2$(N)/C, and $PtSnO_2$(M)/C are 0.203, −0.138, and −0.138 V (*vs*. SCE), respectively. The peak current densities in the three electrodes for ethanol are in the following order: $PtSnO_2$(M)/C > $PtSnO_2$(N)/C > Pt/C, at less than 0.64 V (*vs*. SCE). $PtSnO_2$(M)/C electrode obviously exhibits an extremely high oxidation current density from the quasi-steady-state polarization curves. Two oxidation peaks of ethanol oxidation can be observed on $PtSnO_2$(N)/C and $PtSnO_2$(M)/C catalysts in the range of 0.2 and 0.8 V, which is in accordance with literature results.[8,23] According to the results reported in the literature, the second oxidation peak (0.7 V) corresponds mainly to the formation of CH_3COOH, whereas the first oxidation peak (0.36 V) corresponds mainly to the formation of CH_3CHO. It has been found that CH_3CHO was formed on Pt surface at potentials lower than 0.6 V (*vs*. RHE).[29] As soon as CH_3CHO was formed, it adsorbed on Pt sites and formed CH_3CO species, which blocked the subsequent oxidation of ethanol.[30] SnO_2 provides hydroxy radical species for the oxidation

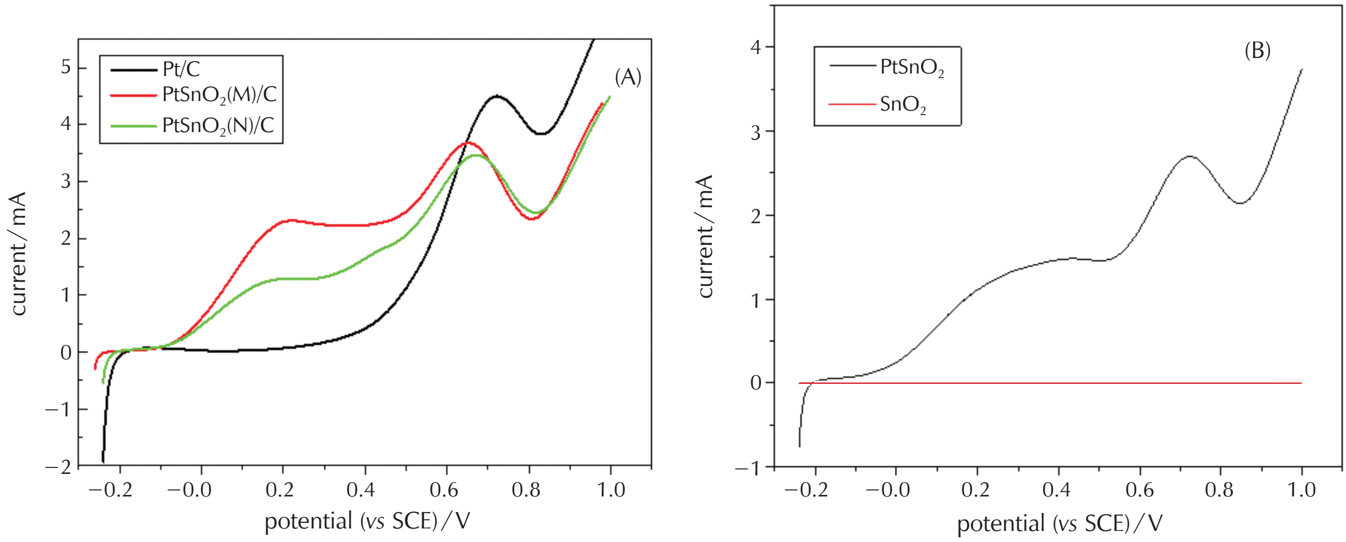

Fig. 7 – (A) LSV of Pt/C, $PtSnO_2$(N)/C, and $PtSnO_2$(M)/C in 0.5 M H_2SO_4 + 1 M EtOH electrolyte at room temperature at a scan rate of 5 mV s^{-1}. (B) LSV of mesoporous SnO_2 and $PtSnO_2$(M)/C in 0.5 M H_2SO_4 + 1 M EtOH electrolyte at room temperature at a scan rate of 5 mV s^{-1}.

of CH_3CHO to CH_3COOH at the potential values below 0.36 V (*vs.* SCE). Because the high activity of mesoporous SnO_2 provides hydroxy radical species for the oxidation of CH_3CHO to CH_3COOH, Pt sites are not blocked. The curve of $PtSnO_2$(M)/C catalyst is found quasi-steady-state polarization in the range of 0.2 and 0.5 V (*vs.* SCE). The LSV of EOR on the SnO_2 and $PtSnO_2$(M) catalyst is also presented (Fig. 7b). Curve SnO_2 shows that mesoporous SnO_2 has no electrocatalytic activity for ethanol oxidation, which is in accordance with literature results.[11] Two oxidation peaks of ethanol oxidation can be observed on $PtSnO_2$(M) catalysts, which is in accordance with $PtSnO_2$(M)/C results in Fig. 7a. According to the results, $PtSnO_2$(M)/C catalysts have better performance due to higher activity of $PtSnO_2$(M). This result also indicated the interaction between Pt and SnO_2.

The catalytic activities and stabilities of Pt/C, $PtSnO_2$(N)/C, and $PtSnO_2$(M)/C electrodes for EOR were investigated *via* CA measurements performed at 0.2 V for 2400 s. The initial high current corresponds mainly to double-layer charging. A steady decrease in current is observed within the first few minutes for the three catalysts, followed by a fairly constant current for a longer period, which may be due to the poisoning effect of CO-like species produced by the continuous oxidation of ethanol on the catalyst surface. In Fig. 8, the final current densities for Pt/C, $PtSnO_2$(N)/C, and $PtSnO_2$(M)/C after maintaining the cell potential are in the following order: $PtSnO_2$(M)/C > $PtSnO_2$(N)/C > Pt/C. The CA curves indicate that the current density of $PtSnO_2$(M)/C is higher than those of $PtSnO_2$(N)/C and Pt/C during the entire time course, thus further verifying that $PtSnO_2$(M)/C exhibits better electrocatalytic performance in ethanol oxidation reaction. The improved anti-poisoning ability of the $PtSnO_2$(M)/C catalysts may be explained by the bifunctional mechanism and high activity of mesoporous SnO_2 providing hydroxy radical species. The results are consistent with LSV measurements.

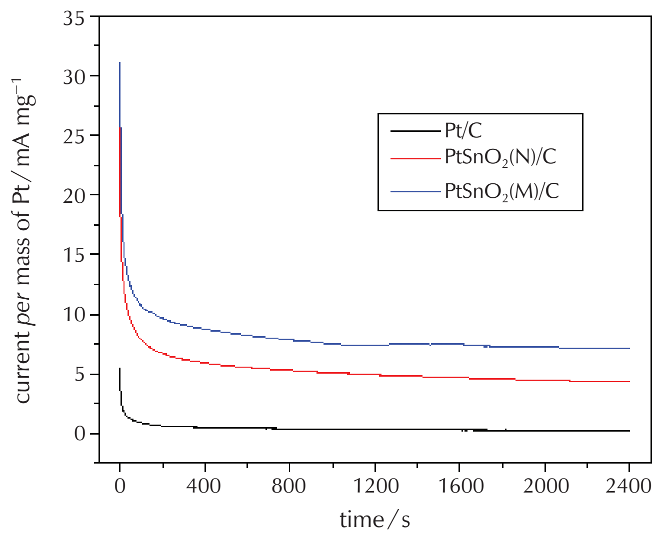

Fig. 8 – Current density – time dependence measured by the CA method in 0.5 M H_2SO_4 + 1 M EtOH electrolyte on Pt/C, $PtSnO_2$(N)/C, and $PtSnO_2$(M)/C electrodes at 0.2 V (*vs.* SCE)

4 Conclusion

In summary, mesoporous SnO_2 was prepared *via* a water-evaporating process. C-supported $PtSnO_2$(M) particles with a nominal Pt : Sn ratio of 3 : 1 were prepared *via* a modified polyol method. As-prepared $PtSnO_2$(M)/C exhibited enhanced electrocatalytic activity toward EOR compared with solid $PtSnO_2$(N)/C and Pt/C catalysts. The enhanced EOR activity could be attributed to the mesoporous structure of SnO_2 and the strong chemical interaction between Pt and SnO_2. This synthesis may lead to new development strategies to prepare EOR catalysts for DEFC.

ACKNOWLEDGEMENTS

This work was supported by the Foundation of Young Scientist of Shihezi University (2013ZRKXJQ03).

List of abbreviations

EOR	– ethanol electro-oxidation reaction
DEFC	– direct ethanol fuel cell
EG	– ethylene glycol
BET	– Brunauer–Emmett–Teller
BJH	– Barrett–Joyner–Halenda
XRD	– powder X-ray diffraction
TEM	– transmission electron microscopy
ICP-AES	– inductively coupled plasma atomic emission spectroscopy
XPS	– x-ray photoelectron spectroscopy
SCE	– saturated calomel reference electrode
LSV	– linear sweep voltammetry
CA	– chronoamperometry
CV	– cyclic voltammetry
ECSA	– electrochemical active surface area
HRTEM	– high resolution transmission electron microscopy

References
Literatura

1. *Y. Lin, S. Zhang, S. Yan, G. Liu*, The effect of Sn content in Pt-SnO_2/CNTs for methanol electro-oxidation, Electrochim. Acta **66** (2012) 1–6, doi: https://doi.org/10.1016/j.electacta.2011.12.109.
2. *W. J. Zhou, S. Q. Song, W. Z. Li, Z. H. Zhou, G. Q. Sun, Q. Xin, S. Douvartzides P. Tsiakaras*, Direct ethanol fuel cells based on PtSn anodes: the effect of Sn content on the fuel cell performance, J. Power Sources **140** (2005) 50–58, doi: https://doi.org/10.1016/j.jpowsour.2004.08.003.
3. *J. C. M. Silva, R. F. B. De Souza, L. S. Parreira, E. T. Neto, M. L. Calegaro, M. C. Santos*, Ethanol oxidation reactions using SnO_2@Pt/C as an electrocatalyst, Appl. Catal. B-Environ. **99** (1-2) (2010) 265–271, doi: https://doi.org/10.1016/j.apcatb.2010.06.031.
4. *M. Li, A. Kowal, K. Sasaki, N. Marinkovic, D. Su, E. Korach, P. Liu, R. R. Adzic*, Ethanol oxidation on the ternary Pt-Rh-SnO_2/C electrocatalysts with varied Pt: Rh: Sn ratios, Electrochim. Acta **55** (2010) 4331–4338, doi: https://doi.org/10.1016/j.electacta.2009.12.071.
5. *M. Li, D. A. Cullen, K. Sasaki, N. S. Marinkovic, K. More, R. R. Adzic*, Ternary electrocatalysts for oxidizing ethanol to carbon dioxide: making Ir capable of splitting C-C bond, J. Am. Chem. Soc. **135** (2012) 132–141, doi: https://doi.org/10.1021/ja306384x.
6. *L. Jiang, G. Sun, S. Sun, J. Liu, S. Tang, H. Li, B. Zhou, Q. Xin*, Structure and chemical composition of supported Pt-Sn electrocatalysts for ethanol oxidation, Electrochim. Acta **50** (2005) 5384–5389, doi: https://doi.org/10.1016/j.electacta.2005.03.018.
7. *H. L. Pang, J. P. Lu, J. H. Chen, C. T. Huang, B. Liu, X. H. Zhang*, Preparation of SnO_2-CNTs supported Pt catalysts and their electrocatalytic properties for ethanol oxidation, Electrochim. Acta **54** (2009) 2610–2615, doi: https://doi.org/10.1016/j.electacta.2008.10.058.
8. *M. Zhu, G. Sun, Q. Xin*, Effect of alloying degree in PtSn catalyst on the catalytic behavior for ethanol electro-oxidation, Electrochim. Acta **54** (2009) 1511–1518, doi: https://doi.org/10.1016/j.electacta.2008.09.035.
9. *W.-P. Zhou, S. Axnanda, M. G. White, R. R. Adzic, J. Hrbek*, Enhancement in ethanol electrooxidation by SnO_x nanoislands grown on Pt (111): effect of metal oxide-metal interface sites, J. Phys. Chem. C. **115** (2011) 16467–16473, doi: https://doi.org/10.1021/jp203770x.
10. *W. Du, G. Yang, E. Wong, N. A. Deskins, A. I. Frenkel, D. Su, X. Teng*, Platinum-Tin oxide core-shell catalysts for efficient electro-oxidation of ethanol, J. Am. Chem. Soc. **136** (2014) 10862–10865, doi: https://doi.org/10.1021/ja505456w.
11. *X. Zhang, H. Zhu, Z. Guo, Y. Wei, F. Wang*, Design and preparation of CNT@SnO_2 core-shell composites with thin shell and its application for ethanol oxidation, Int. J. Hydrogen Energy **35** (2010) 8841–8847, doi: https://doi.org/10.1016/j.ijhydene.2010.05.127.
12. *H. Zhang, C. Hu, X. He, L. Hong, G. Du, Y. Zhang*, Pt support of multidimensional active sites and radial channels formed by SnO_2 flower-like crystals for methanol and ethanol oxidation, J. Power Sources **196** (2011) 4499–4505, doi: https://doi.org/10.1016/j.jpowsour.2011.01.030.
13. *A. Kowal, M. Li, M. Shao, K. Sasaki, M. Vukmirovic, J. Zhang, N. Marinkovic, P. Liu, A. Frenkel, R. Adzic*, Ternary Pt/Rh/SnO_2 electrocatalysts for oxidizing ethanol to CO_2, Nat. Mater. **8** (2009) 325, doi: https://doi.org/10.1038/nmat2359.
14. *Y. Bai, J. Wu, X. Qiu, J. Xi, J. Wang, J. Li, W. Zhu, L. Chen*, Electrochemical characterization of Pt-CeO_2/C and Pt-Ce_x-$Zr_{1-x}O_2$/C catalysts for ethanol electro-oxidation, Appl. Catal. B-Environ. **73** (2007) 144–149, doi: https://doi.org/10.1016/j.apcatb.2006.06.026.
15. *D.-J. Guo, X.-P. Qiu, L.-Q. Chen, W.-T. Zhu*, Multi-walled carbon nanotubes modified by sulfated TiO_2-A promising support for Pt catalyst in a direct ethanol fuel cell, Carbon **47** (2009) 1680–1685, doi: https://doi.org/10.1016/j.carbon.2009.02.023.
16. *G. Chen, Z. Wang, D. Xia*, One-pot synthesis of carbon nanotube@SnO_2-Au coaxial nanocable for lithium-ion batteries with high rate capability, Chem. Mater. **20** (2008) 6951–6956, doi: https://doi.org/10.1021/cm801853c.
17. *P. Manjula, R. Boppella, S. V. Manorama*, A facile and green approach for the controlled synthesis of porous SnO_2 nanospheres: application as an efficient photocatalyst and an excellent gas sensing material, ACS Appl. Mat. Interfaces **4** (2012) 6252–6260, doi: https://doi.org/10.1021/am301840s.
18. *Y. Chen, J. Ma, L. Yu, Q. Li, T. Wang*, Mesoporous SnO_2 nano-

spheres formed *via* a water-evaporating process with superior electrochemical properties, Cryst. Eng. Comm, **14** (2012) 6170–6172, doi: https://doi.org/10.1039/c2ce25769f.

19. *L. Wang, T. Fei, J. Deng, Z. Lou, R. Wang, T. Zhang*, Synthesis of rattle-type SnO_2 structures with porous shells, J. Mater. Chem. **22** (2012) 18111–18114, doi: https://doi.org/10.1039/c2jm32520a.
20. *D. Zhao, B.-Q. Xu*, Platinum covering of gold nanoparticles for utilization enhancement of Pt in electrocatalysts, Phys. Chem. Chem. Phys. **8** (2006) 5106–5114, doi: https://doi.org/10.1039/b610269g.
21. *C. R Parkinson, M. Walker, C. F McConville*, Reaction of atomic oxygen with a Pt (111) surface: chemical and structural determination using XPS, CAICISS and LEED, Surf. Sci. **545** (2003) 19–33, doi: https://doi.org/10.1016/j.susc.2003.08.029.
22. *M. Batzill, U. Diebold*, The surface and materials science of tin oxide, Surf. Sci. **79** (2005) 47–154, doi: https://doi.org/10.1016/j.progsurf.2005.09.002.
23. *C. Hu, Y. Cao, L. Yang, Z. Bai, Y. Guo, K. Wang, P. Xu, J. Zhou*, Preparation of highly dispersed Pt-SnO_x nanoparticles supported on multi-walled carbon nanotubes for methanol oxidation, Appl. Surf. Sci. **257** (2011) 7968–7974, doi: https://doi.org/10.1016/j.apsusc.2011.04.010.
24. *K. Ke, K. Waki*, Fabrication and Characterization of Multi-walled Carbon Nanotubes-Supported Pt/SnO_x Nanocomposites as Catalysts for Electro-oxidation of Methanol, J. Electrochem. Soc. **154** (2007) A207–A212, doi: https://doi.org/10.1149/1.2426873.
25. *R. Liu, S. Yang, F. Wang, X. Lu, Z. Yang, B. Ding*, Sodium chloride template synthesis of cubic tin dioxide hollow particles for lithium ion battery applications, ACS Appl. Mat. Interfaces **4** (2012) 1537–1542, doi: https://doi.org/10.1021/am201756m.
26. *G. Neri, C. Milone, S. Galvagno, A. P. J. Pijpers, J. Schwank*, Characterization of Pt-Sn/carbon hydrogenation catalysts, Appl. Catal. A **227** (2002) 105–115, doi: https://doi.org/10.1016/S0926-860X(01)00927-9.
27. *E. P. Lee, Z. Peng, D. M. Cate, H. Yang, C. T. Campbell, Y. Xia*, Growing Pt nanowires as a densely packed array on metal gauze, J. Am. Chem. Soc. **129** (2007) 10634–10635, doi: https://doi.org/10.1021/ja074312e.
28. *Y. Du, B. Su, N. Zhang, C. Wang*, A novel preparation method of Sn-modified Pt nanoparticles and application for methanol oxidation, Appl. Surf. Sci. **255** (2008) 2641–2645, doi: https://doi.org/10.1016/j.apsusc.2008.07.147.
29. *H. Hitmi, E. M. Belgsir, J.-M. Léger, C. Lamy, R. O. Lezna*, A kinetic analysis of the electro-oxidation of ethanol at a platinum electrode in acid medium, Electrochim. Acta. **39** (1994) 407–415, doi: https://doi.org/10.1016/0013-4686(94)80080-4.
30. *F. Vigier, C. Coutanceau, F. Hahn, E. M. Belgsir, C. Lamy*, On the mechanism of ethanol electro-oxidation on Pt and PtSn catalysts: electrochemical and in situ IR reflectance spectroscopy studies, J. Electroanal. Chem. **563** (2004) 81–89, doi: https://doi.org/10.1016/j.jelechem.2003.08.019.

SAŽETAK

Mezoporozni katalizator $PtSnO_2$/C s povećanom katalitičkom aktivnošću za elektrooksidaciju etanola

Siyu Chen,[a] *Lei Shi* [a,b*] i *Liang Wang* [c]

U ovom radu prikazana je sinteza, karakterizacija i elektrokemijska ocjena mezoporoznog katalizatora $PtSnO_2$/C ($PtSnO_2$(M)/C), s nominalnim omjerom Pt : Sn od 3 : 1. Karakterizacije Brunauer-Emmett-Tellerovom metodom i transmisijskom elektronskom mikroskopijom pokazale su očitu mezoporoznu strukturu SnO_2 u katalizatoru $PtSnO_2$(M)/C. Analiza rendgenskom fotoelektronskom spektroskopijom pokazala je interakciju između Pt i mezoporoznog SnO_2. U usporedbi s Pt/C i komercijalnim katalizatorima $PtSnO_2$/C, katalizator $PtSnO_2$(M)/C ima slabije aktivno mjesto, ali veću katalitičku aktivnost za reakciju elektrooksidacije etanola (EOR). Poboljšana aktivnost mogla bi se pripisati nanočesticama Pt pohranjenim na mezoporoznom SnO_2, što bi moglo smanjiti količinu otrovnih međuprodukata proizvedenih tijekom elektrooksidacije etanola interakcijom između Pt i mezoporoznog SnO_2.

Ključne riječi
Reakcija elektrooksidacije etanola, katalizator Pt-Sn, mezoporozni SnO_2, pojačana katalitička aktivnost

[a] *School of Chemistry and Chemical Engineering, Shihezi University, Shihezi, Xinjiang, 832 000, Kina*
[b] *Key Laboratory for Green Processing of Chemical Engineering of Xinjiang Bingtuan, Shihezi, Xinjiang, 832 000, Kina*
[c] *Shandong University of Traditional Chinese Medicine, Shandong, 250 355, Kina*

Izvorni znanstveni rad
Prispjelo 3. srpnja 2017.
Prihvaćeno 27. listopada 2017.